Renewable Energy 227 (2024) 120547

Contents lists available at ScienceDirect

Renewable Energy

journal homepage: www.elsevier.com/locate/renene

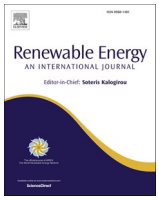

Improvements in dewaterability and fuel properties of hydrochars derived from hydrothermal co-carbonization of sewage sludge and organic waste

Małgorzata Wilk *, Maciej Śliz, Klaudia Czerwińska, Marcin Gajek, Izabela Kalemba-Rec

AGH University of Krakow, Mickiewicza 30 Av., 30-312, Krakow, Poland

ARTICLE INFO

Keywords:
Hydrothermal co-carbonization
Sewage sludge
Organic waste
Hydrochar
Dewaterability
Fuel properties

ABSTRACT

The hydrothermal co-carbonization of sewage sludge and organic additives, namely 10 and 20 % of charcoal, fir, grass, and an undersieved fraction of municipal solid waste, was studied. The benefits of this combined process included the spectacular dewaterability performance of slurry, proved by positive filtration tests and shorter capillary suction times. For instance, a 20 % fir addition decreased c.a. 60 % of pressure filtration time when compared to the hydrothermal carbonization of sewage sludge. A 10 % undersieved fraction of municipal solid waste resulted in 15.72 s of capillary suction time. Moreover, hydrothermal co-carbonization produced effective solid energy sources. The addition of organic origin waste to sewage sludge prior to the process caused higher heating values, carbon and fixed carbon contents of hydrochars (e.g. a 20 % charcoal addition generated 21 % higher heating value, 30 % carbon and 2.8 times higher fixed carbon), which corresponded with easier and more stable combustion processes compared to hydrochar from sewage sludge determined by thermal analysis. Possible exploitation problems during combustion have been assessed by determining the tendency risks of slagging and fouling based on oxides identified in ash by XRF analysis. Furthermore, changes in the structural and morphological properties of hydrochars were identified by SEM and FTIR analyses.

1. Introduction

The hydrothermal carbonization process (HTC) is among the "sludge-to-energy" (StE) technologies which are in line with the circular economy concept [1–4]. It aims to reduce the volume of waste, reuse novel products and limit waste in landfilling. HTC is carried out in an aqueous environment under heat and pressure and results in solid (hydrochar), liquid and gaseous products which might be further used as biofuels, biofertilizers or adsorbents [5,6]. Due to the fact that HTC is dedicated to wet feedstocks, sewage sludge (SS) with a high moisture content (c.a. 80 %) and of an organic origin is an appropriate material to process [7,8].

This technique indeed decreases the volume of sewage sludge, greatly improves its dewaterability and reduces nitrogen and sulphur contents resulting in significantly lower costs for the predrying of hydrochar and a reduction of pollutant emission concerning sewage sludge application in the combustion process [9–11]. Moreover, the range of temperatures used during this hydrothermal conversion (180–250 °C) enables the deactivation of pathogens, bacteria and viruses contained in sewage sludge [12].

Unfortunately, SS contains a high content of inorganic matter, thus the ash content after the combustion process is high and higher still when the HTC process is applied. This is due to an excess loss of volatile matter and retention of minerals [13]. The high ash content affects the fuel properties of hydrochar derived from the HTC of SS. Although hydrochar qualifies for energy purposes [14], it is expected to have better combustible properties.

A promising option to enhance its fuel properties and minimize the ash content is the hydrothermal co-carbonization of sewage sludge and some organic additives. For instance, Wilk et al. [15] reported the upgrading of fuel properties in hydrochars from blends derived from SS and fuel additives and significant improvements in the dewaterabitity of sewage sludge. Lu et al. [16] investigated mixtures of SS and cellulose, xylan or lignin in order to assess their fuel properties and lower heavy metal (HM) contents in ash. This team also investigated hydrochar derived from SS and pinewood and stated that the co-HTC lowered HM contents and moreover an additional treatment with citric acid exhibited the lowest potential ecological risk [17]. Additionally, the heavy metal contamination and fuel properties of hydrochars from the co-hydrothermal carbonization of sewage sludge and banana stalk were studied by mathematical models to reveal the relationship between

* Corresponding author.
E-mail address: mwilk@agh.edu.pl (M. Wilk).

https://doi.org/10.1016/j.renene.2024.120547
Received 2 January 2024; Received in revised form 16 April 2024; Accepted 21 April 2024
Available online 22 April 2024

Nomenclature

BAI	bed agglomeration index
C	carbon content, %
C	charcoal
C_6H_5OH	phenol
Ca	Calcium, mg/L
Cl	chlorine free, mg/L
COD	chemical oxygen demand, mg/L
co-HTC	hydrothermal co-carbonization
CST	capillary suction time, s
D_b	burnout index, %/min^4
D_i	ignition index, %/min^3
DOM	dry organic matter, %
DSC	differential scanning calorimetry
DTG	differential thermogravimetric
DTG_{mean}	mean weight loss rate 1, %/min
DTG_{max}	maximum combustion rate 1, %/min
DTG_1	weight loss rate 1, %/min
DTG_2	weight loss rate 2, %/min
F	fir
FC	fixed carbon content, %
F_U	fouling index
G	grass
FTIR	Fourier-transform infrared spectroscopy
H	hydrogen content, %
H_f	combustion stability index, °C
HHV	high heating value, MJ/kg
HM	heavy metal
HTC	hydrothermal carbonization
HTC_SS	hydrothermal carbonization of sewage sludge
HTC_1C	hydrothermal carbonization of sewage sludge and 10 % charcoal
HTC_2C	hydrothermal carbonization of sewage sludge and 20 % charcoal
HTC_1F	hydrothermal carbonization of sewage sludge and 10 % fir
HTC_2F	hydrothermal carbonization of sewage sludge and 20 % fir
HTC_1G	hydrothermal carbonization of sewage sludge and 10 % grass
HTC_2G	hydrothermal carbonization of sewage sludge and 20 % grass
HTC_1U	hydrothermal carbonization of sewage sludge and 10 % undersieved fraction of municipal solid waste
HTC_2U	hydrothermal carbonization of sewage sludge and 20 % undersieved fraction of municipal solid waste
HSS	hydrochar of sewage sludge
H1C	hydrochar of sewage sludge and 10 % charcoal
H2C	hydrochar of sewage sludge and 20 % charcoal
H1F	hydrochar of sewage sludge and 10 % fir
H2F	hydrochar of sewage sludge and 20 % fir
H1G	hydrochar of sewage sludge and 10 % grass
H2G	hydrochar of sewage sludge and 20 % grass
H1U	hydrochar of sewage sludge and 10 % undersieved fraction of municipal solid waste
H2U	hydrochar of sewage sludge and 20 % undersieved fraction of municipal solid waste
HSSL	process water derived from hydrothermal carbonization of sewage sludge
H1CL	process water derived from hydrothermal carbonization of sewage sludge and 10 % charcoal
H2CL	process water derived from hydrothermal carbonization of sewage sludge and 20 % charcoal
H1FL	process water derived from hydrothermal carbonization of sewage sludge and 10 % fir
H2FL	process water derived from hydrothermal carbonization of sewage sludge and 20 % fir
H1GL	process water derived from hydrothermal carbonization of sewage sludge and 10 % grass
H2GL	process water derived from hydrothermal carbonization of sewage sludge and 20 % grass
H1UL	process water derived from hydrothermal carbonization of sewage sludge and 10 % undersieved fraction of municipal solid waste
H2UL	process water derived from hydrothermal carbonization of sewage sludge and 20 % undersieved fraction of municipal solid waste
HM	heavy metal content
Kjeldahl N	Kjeldahl nitrogen, mg/L
Mg	magnesium, mg/L
NH_4^+	ammoniacal nitrogen, mg/L
N	nitrogen content, %
O	oxygen content, %
PO_4-P	orthophosphate, mg/L
PO_4^{-3}	phosphate, mg/L
P_2O_5	phosphorus pentoxide, mg/L
R	solid residue, %
R_B	basic constituents index
$R_{B/A}$	base-to-acid index
R_S	slagging index
S	sulphur content, %
S	comprehensive combustion index, %^{2}/(min^2·°C^3)
S	type of thermocouple
S_R	slag viscosity index
SEM	scanning electron microscope
SS	sewage sludge
SSA	specific surface area, m^2/g
t_b	burnout time, min
t_i	Ignition time, min
t_1	corresponding time for DTG_1, min
t_2	corresponding time for DTG_2, min
total Cl	total chlorine, mg/L
total P	total phosphorus, mg/L
T_b	burnout temperature, °C
T_i	ignition temperature, °C
T_1	temperature at DTG_1, °C
T_2	temperature at DTG_2, °C
TG	thermogravimetric analysis
TGA	thermal analysis
TOC	total organic carbon, mg/L
U	undersieved fraction of municipal solid waste
WD-XRF	Wavelength Dispersive X-ray Fluorescence
VM	volatile matter content, %
XRF	X-ray fluorescence analysis
$\Delta t_{0.5}$	time range of $DTG/DTG_1 = 0.5$, min

hydrochar properties and process parameters and to confirm that positive synergistic effects of banana stalk addition were mainly caused by Maillard and Mannich reactions, leading to the upgradation of hydrochar fuel properties [18]. Furthermore, Zhang et al. [19] discovered that SS and pinewood sawdust resulted in synergistic effects and improved hydrochar for combustion. The same conclusions regarding the advantageous role of additives were revealed by He et al. [20] and Peng et al. [21] who examined hydrochars derived from sewage sludge and fruit, lignocellulosic or agriculture wastes. Wang et al. [22] studied hydrochar from SS and cornstalk and achieved the greatest higher heating value at

220 °C and 2h besides the study of redistribution, migration and the pathway mechanism of nitrogen in this blend. Hydrothermal co-carbonization of cornstalk and sawdust was studied by Wang et al. [23] who connected this technique with the anaerobic digestion of wastewater to optimize the energy yield of this process. In addition, Parmar et al. [24] followed this concept and investigated the influence of blending sewage sludge and green waste on HTC product quality including the combustion performance of hydrochar and biomethane potential of process water. Djandja et al. [25] applied machine learning prediction to estimate the carbon content, O/C, higher heating value, mass and energy yields as well as fuel ratio of SS and different types of biomass origin including lignocellulosic, agro- and food waste residues. Finally, Bardhan et al. [26] and Fakudze et al. [27] summarized in their review that the synergistic effects of feedstock types, blending ratio, temperature, and residence time upgraded HHV and the chemical and physical properties of hydrochars in terms of fuel production.

The liquid phase, resulting from the hydrothermal carbonization process of sewage sludge, is a highly intricate major by-product containing inorganic and a significant load of organic substance proved by its high total organic carbon and chemical oxygen demand values. These are mainly carbohydrates, protein, and short-chain organic acids, e.g. acetic, propionic, benzenoacetic and butanoic acids, phenolic, furanic, alkene, aromatic, and aldehydic compounds, dissolved organic matter, nitrogen, phosphorus and potassium. The properties of process water are greatly influenced by the operating conditions of the HTC process mainly temperature, residence time, solid loadings, origin of feedstock and pH environment and as well as the additives used. For instance, depending on the additives applied, the pH of process water varies from alkaline to acidic, from 7 to 8 for SS alone [9] to c.a. 6 for hyacinth [28] or c.a. 3.5 for lignocellulosic biomass [24], which influences the decomposition of organic matter, followed by the distribution and amount of micro- and macronutrients such as phosphorous, nitrogen or potassium [29]. The presence of these elements in the process water indicates that it might be applied as a potential liquid fertilizer [30]. Therefore, knowledge of process water properties derived from the hydrothermal co-carbonization process is essential before its proper disposal.

This study is focused on the dewaterability performance of slurries from the hydrothermal co-carbonization of sewage sludge and organic waste and the combustion behaviour of hydrochars. State-of-the-art treatment was previously focused primarily on the fuel properties of hydrochar rather than the ability of additives to enhance the removal of water from sewage sludge. The research team had already investigated the topic, but now presents a more advanced detailed description of these simultaneous behaviours for 10 and 20 % of organic waste additives with sewage sludge during hydrothermal co-carbonization.

Accordingly, the filtration tests and capillary suction tests were applied in order to study and discuss the dewaterability performance. Additionally, the ultimate and proximate analyses, and higher heating values were supported by the TGA of hydrochars to assess the influence of the additives on their fuel properties. Furthermore, SEM, FTIR, and SSA analyses were employed to study the changes in the structure of hydrochars and to assess the sorptive properties of hydrochars. In addition, the main characteristics of process water were determined.

2. Materials and methods

2.1. Materials

This study is a continuation of the previous work reported in Ref. [15], where sewage sludge with 10 % of fuel additives, including charcoal, oak sawdust and fir sawdust (10 and 20 %), were investigated under hydrothermal co-carbonization The best fuel properties were found for hydrochar derived from sewage sludge with 20 % fir sawdust. Based on these trends the following additives: fir sawdust, grass, charcoal and an undersieved fraction of municipal solid waste at amounts of 10 and 20 % were studied in terms of the combustion performance of hydrochars.

Digestated sewage sludge (SS) was collected from Żory Wastewater Treatment Plant, where it was dewatered to 83.21 % of moisture content by filtration press. For the purpose of the hydrothermal tests it was diluted by distilled water to 90 % of moisture content to enable easy stirring of feedstock in the HTC reactor.

Fir (F) was supplied from the Beskidy mountain plantation [15]. Grass (G) was supplied from the Żory Wastewater Treatment Plant terrain. Both lignocellulosic additives were air dried and milled to below 1 mm. The charcoal (C) was a commercial product, which was ground in a roller mill below 0.2 mm. The undersieved fraction of municipal solid waste (U) was collected from an Italian MTB plant in the metropolitan area of Florence (central Italy) [31] after metal recovery.

2.2. Methods

2.2.1. Hydrothermal carbonization process

The hydrothermal carbonization process was performed in a 1 L volume Zipperclave Stirred Reactor, Parker Autoclave Engineers, USA. The 700 mL of feedstock was inserted into the reactor and heated to 200 °C, then it was maintained for 2 h. The optimal conditions of the hydrothermal carbonization process have been carefully revised by the research team [12] and used in the previous work on this topic [15]. In this work, the same conditions were applied to achieve a better comparison of these results. When the time of reaction was over, the heating jacket was removed and the reactor was cooled down by cooling water via a cooling coil and by ice box. Then, the slurry was evacuated from the reactor and solid and liquid products were separated by filtration apparatus. The hydrochars were dried at 105 °C and stored for further analyses.

Hydrochar derived from the sewage sludge was named HSS, whereas hydrochars from hydrothermal co-carbonization were labelled in the following way: the first letter was H – representing hydrochar, and was followed by numbers 1 or 2 – representing 10 and 20 % of each of the additives, then was a consecutive letter representing the additives, namely C – charcoal, F – fir sawdust, G – grass, and U – under sieved fraction of municipal solid waste. For instance, H1F portrayed hydrochar derived from the hydrothermal co-carbonization of sewage sludge with 10 % of fir sawdust.

2.2.2. Dewaterability

The dewaterability performance was carried out by the capillary suction time tests (CST) and filtration tests according to the procedure described in Ref. [15]. In brief, CST was conducted according to EN 14701–1:2006 with a CST meter with a cylinder diameter of 18 mm and height of 25 mm and filtration paper (Whatman 17). The filtration tests were determined by a hydraulic pressure unit to achieve the lowest moisture content of filtration cake. Firstly, the filtration of 150 mL of slurry with a constant pressure at 4 bars was applied, then after the filtrate stopped to leak the 16 bar were used for final compression of filtration cake.

2.2.3. Fuel properties

The proximate and ultimate analyses were performed according to European standards. The moisture content was measured according to ISO 18134–2:2017. Ash content was determined according to ISO 18122:2022, whereas volatile matter content was according to ISO 18123:2023. The ultimate analysis, including carbon, hydrogen, nitrogen, and sulphur contents, was determined according to ISO 29541:2010, employing the Elemental Analyser Truespec CHNS 628 Leco, USA. The high heating value (HHV) was performed in a Leco AC500 isoperibolic calorimeter.

Thermal analysis was conducted in an air atmosphere (40 mL/min) within the range, 10°/min heating rate up to 700 °C, with a Netzsch STA 449 F3 Jupiter using a standard DSC/TG sample carrier (thermocouples

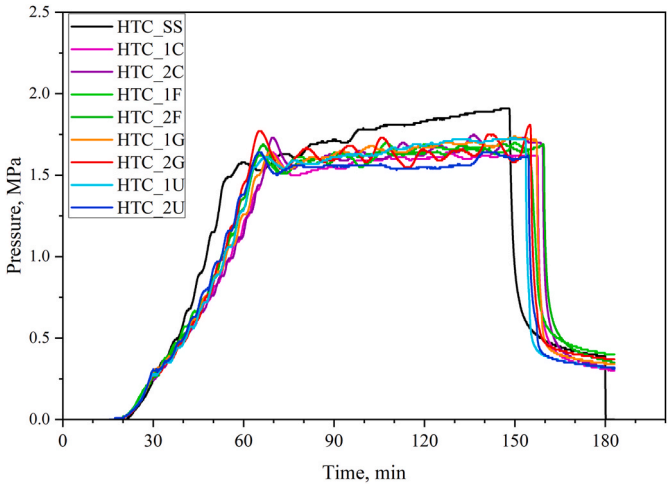

Fig. 1. Recorded pressure for hydrothermal carbonization tests with and without additives.

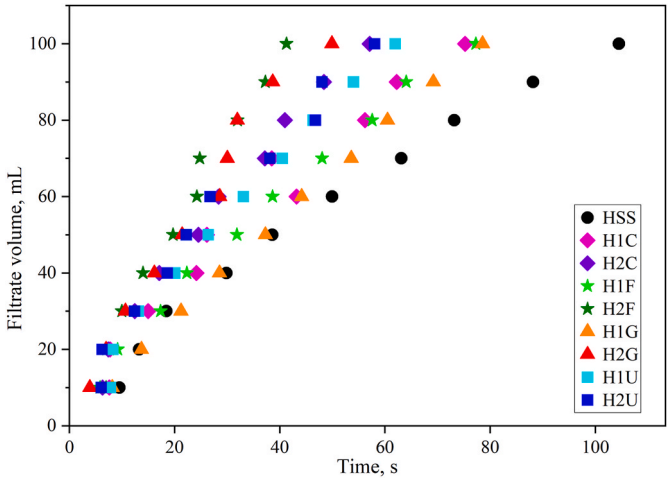

Fig. 2. Filtration tests for hydrothermal slurries.

type S) to simulate the combustion process of hydrochar.

Ash of sewage sludge and organic waste additives may cause the exploitation problems during combustion, which was the reason for its chemical composition being measured. For this purpose, the X-ray fluorescence method (WD-XRF) was applied using a WD-XRF ZSX Primus II Rigaku spectrometer (Rh lamp) to identify oxides in ash. Consequently, this enabled the calculation of the following indices: slag viscosity (S_R), basic constituents (R_B), base-to-acid ($R_{B/A}$), bed agglomeration during fluidized combustion (BAI), slagging (R_S), and fouling (F_U).

Table 1
The CST of sewage sludge and HTC slurry, final volume of filtrated liquids and moisture contents of cakes from pressure filtration.

	CST s	Volume of filtrate mL	Moisture content %
SS	8682	7	89
HSS	19.49	125.86	52.62
H1C	19.11	128.52	47.40
H2C	17.76	128.40	47.29
H1F	21.89	123.98	51.00
H2F	17.51	123.06	51.27
H1G	20.48	134.21	45.40
H2G	17.97	132.55	48.78
H1U	15.72	127.11	48.28
H2U	16.29	129.36	46.20

2.2.4. Material properties

Morphological structure analysis and identification of chemical elements were performed by scanning electron microscope (SEM) using FESEM Nova NanoSEM 450, Zeiss, Germany. The functional group was identified by Fourier Transform Infrared (FTIR) using Bruker Alpha II spectrometer, Germany, in the 400–4000 cm^{-1} range of the infrared absorption frequency.

Additionally, the specific surface area of the materials was measured by the Brunauer–Emmett–Teller multipoint adsorption method employing the ASAP 2010 apparatus, Micromeritics Inst. Prior to tests the samples were degassed at 200 °C for 24 h and then the tests were processed at 77 K using nitrogen as the adsorbate. In addition, the polarity index (O + N)/C [32], which exemplifies the hydrophobicity of the organic feedstocks, was determined based on ultimate and proximate analysis [31].

2.2.5. Process water characteristics

The process water derived from the hydrothermal carbonization of sewage sludge (HSSL) and hydrothermal co-carbonization, was labelled, with emphasis on the amount and kind of additives and their liquid state, namely: H1CL, H2CL, H1FL, H2FL, H1GL, H2GL, H1UL, and H2UL.

The following parameters were characterized. Electrical conductivity and pH were measured by the multifunctional analyzer CPC 505 using the Elmetron, Poland. A spectrophotometer Merck Spectroquant Pharo 100 and a Thermoreactor Merck Spectroquant® Series TR 620, Germany were employed to determine the following parameters: chemical oxygen demand (COD), total organic carbon (TOC), ammoniacal nitrogen (NH_4^+), Kjeldahl nitrogen (Kjeldahl N), total nitrogen (total N), total phosphorus (total P), phenol (C_6H_5OH), magnesium (Mg), calcium (Ca), chlorine free (free Cl), and chlorine total (total Cl).

3. Results

During the hydrothermal carbonization of sewage sludge and co-carbonization of sewage sludge and organic waste, the pressure of the process was recorded online simultaneously with the temperature of the process for all tests. The set temperature of the processes was programmed at 200 °C. According to Fig. 1, the organic waste additives caused a decrease in the pressure compared to the HTC of sewage sludge indicating that the set temperature for HTC with additives was achieved later. The pressure of the HTC of sewage sludge test started and finished earlier and had an increasing profile from c.a. 1.5–19.1 MPa, whereas for the additives the pressure profile was more stabilized at c.a. 1.60 MPa. The maximum recorded pressures for all HTC tests were as follows: HTC_SS – 1.91 MPa, HTC_1C – 1.64 MPa, HTC_2C – 1.73 MPa. HTC_1F – 1.70 MPa, HTC_2F – 1.69 MPa, HTC_1G – 1.73 MPa, HTC_2G – 1.81 MPa, HTC_1U – 1.73 MPa, and HTC_2U – 1.64 MPa.

The dried hydrochars derived from hydrothermal co-carbonization were dark brown in colour despite the amount of different additives. In the case of using charcoal as an additive the colour was darker. It was easier to grind in comparison to raw sewage sludge and organic waste and had smaller particles. Additionally, the bulk density was higher than for feedstock.

The dewaterability performance of slurry from hydrothermal carbonization process of sewage sludge without and with organic waste was discussed by comparing the filtration tests from pressure filtration unit and capillary suction times (Fig. 2 and Table 1). Sewage sludge was indeed very difficult to dewater which was proved by collecting only 7 mL of filtrate after pressure filtration and a very long measured capillary suction time in CST meter. In contrary, after hydrothermal carbonization process the capillary suction time, final volume of filtrate and filtration curve were greatly improved. Moreover, the moisture content of cakes from pressure filtration were halve lower in comparison to

Table 2
The ultimate analyses of feedstocks and hydrochars, db.

	C %	H %	N %	S %	O %	(O + N)/C
SS	36.9	5.50	5.99	1.57	19.98	0.55
C	77.8	3.69	0.66	0.06	11.35	0.12
F	47.5	6.31	0.39	0.00	44.83	0.71
G	39.8	5.70	2.43	0.00	31.23	0.64
U	43.3	6.22	1.23	0.00	18.65	0.35
HSS	35.3	4.69	3.36	1.23	10.81	0.31
H1C	41.1	4.40	3.27	1.14	10.71	0.26
H2C	45.6	4.31	3.08	1.09	10.47	0.23
H1F	36.5	4.63	3.53	1.19	11.22	0.31
H2F	37.3	4.63	3.52	1.16	12.40	0.33
H1G	36.5	4.63	3.53	1.19	11.22	0.31
H2G	37.3	4.63	3.52	1.16	12.40	0.33
H1U	35.3	4.69	3.36	1.23	10.81	0.31
H2U	36.7	4.62	3.29	1.15	11.26	0.31

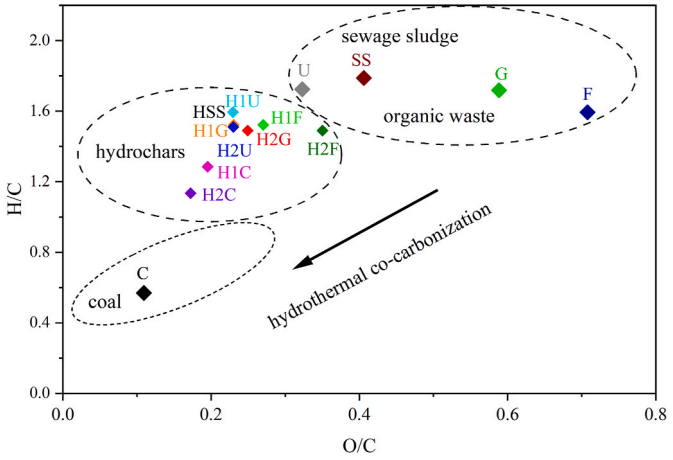

Fig. 3. Van Krevelen diagram.

sewage sludge.

Regarding, the organic waste additives to sewage sludge prior to hydrothermal carbonization, it was found that they enhanced the time of pressure filtration, in particular with 20 % of additives. The curves for H2F presented the most promising decrease (c.a. 60 %) of pressure filtration time. Similarly H2G, H2C and H2U followed the same trends. From the other hand, in the case of H2F, the least filtrate from pressure filtration was collected and the moisture content in filtration cake was c. a. 51 %. The lowest moisture content and the greater volume of filtrate was found for H1G.

Regarding, the CST of hydrothermal co-carbonized slurry, the shortest times were achieved for 20 % of additives with one exception, a 10 % of undersieved fraction of municipal solid waste, which took 15.72 s. The time of hydrothermally carbonized sewage sludge was also short proving that this method is a good option for improvements in sewage sludge dewaterability.

The chemical properties of hydrochars derived from sewage sludge and feedstocks are summarized in Table 2 and depicted in a van Krevelen diagram (Fig. 3).

The ultimate analyses of sewage sludge and origin waste additives were included in Table 2 for comparison. The highest content of carbon was found for charcoal, fir sawdust, undersieved fraction of municipal solid waste, grass and sewage sludge. In the case of hydrogen content, the highest content was in fir, undersieved fraction of municipal solid waste, grass and charcoal. The highest content of oxygen was measured for fir sawdust. Nitrogen content was almost 5 times higher in sewage sludge than in lignocellulosic waste, and fir. However, with grass, the amount was 2 times higher. It is also worth mentioning that in sewage

Table 3
The proximate analyses, dry organic matter content, and fuel ratio supported by higher heating value of feedstocks and hydrochars, db.

	FC%	VM%	Ash%	DOM%	FC/VM	HHVMJ/kg
SS	8.52	61.42	28.04	71.96	0.14	16.31
C	66.07	27.49	3.14	96.86	2.40	30.49
F	17.59	81.44	0.97	99.03	0.22	17.66
G	9.25	69.91	16.71	83.29	0.13	15.86
U	6.63	62.77	30.6	69.40	0.11	17.29
HSS	9.21	46.18	44.61	55.39	0.20	15.58
H1C	18.09	42.53	39.38	60.62	0.43	17.37
H2C	25.92	38.64	35.44	64.56	0.67	18.83
H1F	13.35	45.66	40.99	59.01	0.29	16.33
H2F	14.92	49.11	35.97	64.03	0.30	17.09
H1G	10.89	46.18	42.93	57.07	0.24	15.96
H2G	11.40	47.61	40.99	59.01	0.24	16.14
H1U	9.21	46.18	42.98	57.02	0.22	16.05
H2U	10.15	48.72	41.02	58.98	0.21	16.32

sludge sulphur and nitrogen are found which has be taken into in regard to when it will be disposed by the combustion process.

Regarding hydrochars from hydrothermal co-carbonization, their carbon contents were more or less the same or slightly higher than hydrochar from sewage sludge (HSS) except for blends prepared with charcoal (H1C and H2C) in which carbon contents were 30 % higher. The remaining elements had similar contents: hydrogen was in the range 4.31–4.69 %, nitrogen was close to 3.53–3.08 %, and oxygen c.a. 12.40–10.81 %. The sulphur content was close to the sewage sludge amount c.a. 1.2 %. It can be stated that the hydrochars from blends of sewage sludge and origin waste additives have a relatively uniform chemical composition which remains much closer to sewage sludge than to the additives' properties. Only in the case of charcoal is the difference more noticeable. This is also confirmed by the visual presentation of chemical changes in hydrochar depicted in the van Krevelen diagram, where the hydrochars molar ratios are found in the central zone of the figure, which has shifted to the left side of the figure in the direction of coal, where charcoal chemical properties belong.

The polarity index, e.g. the molar fraction of (O + N)/C [33], expresses the hydrophobicity of organic material. According to Li et al. [34] the most hydrophobic properties is found for feedstock with a smaller value of polarity index. Therefore, it could be stated that the polarity index confirms the positive impact of hydrothermal carbonization and co-carbonization on sewage sludge as well as enhancement of its hydrophobicity and dewaterability. Moreover, the values of the polarity index are quite similar for most of the studied hydrochars, excluding those with charcoal addition which presented with an even smaller value, thereby confirming uniformity of hydrochar properties.

The proximate analyses of hydrochars also follow these trends and are more similar to the reference sample (HSS) (Table 3). Unfortunately, after hydrothermal carbonization and co-carbonization a higher amount of ash (35–45 %) was found in hydrochars than in sewage sludge [35] mainly because mineral matter accumulated in the samples during reactions under temperature and pressure in the aquatic environment [36]. According to the data shown in Table 3, hydrothermal treatment decreased the volatile matter content of sewage sludge. The highest fixed carbon and fuel ratio was determined for a blend of sewage sludge and 20 % of charcoal which strictly corresponded with its higher heating values results (18.83 MJ/kg) and the highest fuel ratio (FC/VM). It is probably due to the larger content of lignin and also of skeleton made by lignocellulosic biomass, having porous structure, leading to formation of secondary char e.g. fixed carbon [27]. According to the Journal of Laws of the Republic of Poland published by the Ministry of the Climate and Environment (January 4, 2023) [37], sewage sludge is adequately stabilized if its dry organic matter (DOM) is reduced by at least 38 %. Taking into account the average moisture content in sludge is at a level of 75 %, the average dry matter content is 65 % [38]. Table 3 presents the DOM contents of hydrochars (55–65 %), which are much less than in

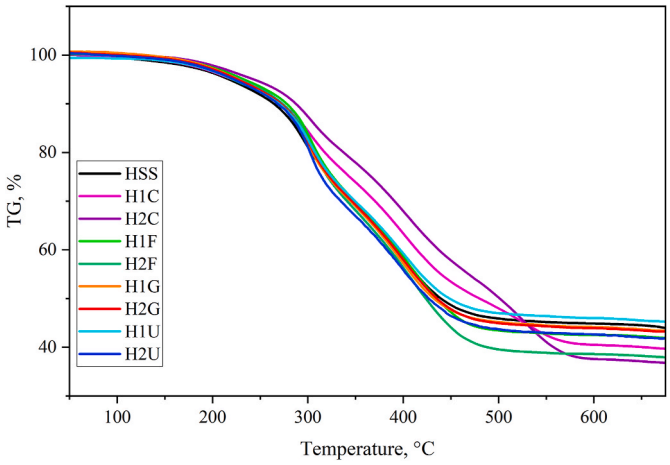

Fig. 4. TG of hydrochars.

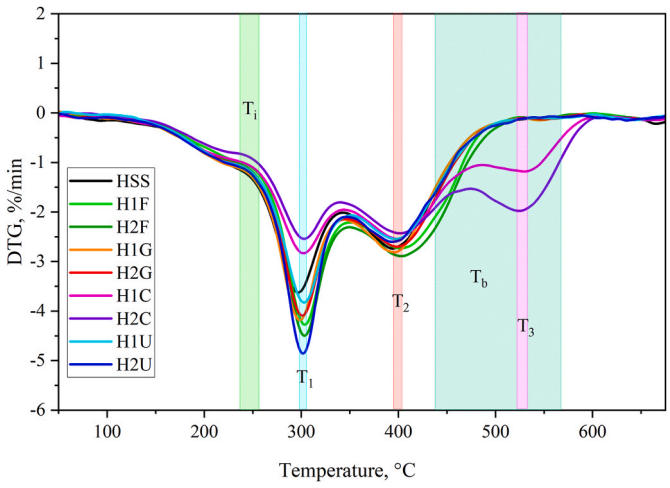

Fig. 5. DTG of hydrochars.

sewage sludge (c.a. 72 %), and confirms that hydrothermal carbonization and its co-carbonization process is a proper method of sewage sludge treatment.

Thermal analysis was applied to hydrochars in order to study the performance of the combustion process. The thermogravimetric profiles are depicted in Fig. 4 to distinguish the stages of the combustion process. The first stage refers to release of moisture content. However, in the case of hydrochars, it is not clearly visible due to the drying process prior to TGA and the hydrophilic nature of hydrochars. The second stage consisted of two parts: volatile matter release and combustion (259–350 °C) and char combustion (350–570 °C). The process was over when any changes were observed in the mass of solid residue. The combustion profiles of hydrochars confirmed the observation concluded previously.

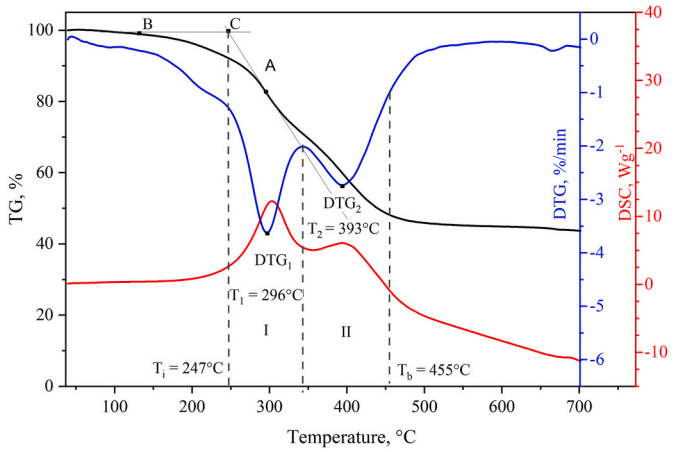

Fig. 6. TGA characteristics for HSS sample.

Most of the hydrochars combusted similarly with the second combustion stage at 250–450 °C with only two exceptions: the hydrochars with charcoal, which combusted for a longer time and at higher range of temperatures (H1C and H2C) [15].

DTG profiles confirm these observations (Fig. 5). The first peak indicating the majority of hydrochars was found at c.a. 300 – 320 °C, followed by the second at c.a. 400 °C. The samples with fir sawdust behaved slightly differently and its DTG profile shifted towards higher temperatures. Additionally, the DTG profiles differed for hydrochars with charcoal and presented third peaks c.a. 530 °C.

Based on the TG and DTG curves, the main characteristics, temperatures and indexes were determined (Table 4) as it is depicted in Fig. 6, and presented as an example for HSS sample [12,15,39].

For instance, ignition of hydrochar based on the determined temperature ignition (T_i) occurred slightly lower when grass, charcoal and the undersieved fraction of municipal solid waste was added to sewage sludge, but for fir sawdust and 20 % of H2U it was higher with over 250 °C temperatures found (Fig. 5). Regarding burnout temperatures (T_b), representing the end of the combustion process, these are in the range of 455–566 °C. Hydrochar without and with undersieved fraction of municipal solid waste and 10 % of straw are at the same level (455 °C), and for fir additives, they are higher at about 20 K. These values are relatively low indicating a lack of unburnt compounds. In the case of 20 % of straw and charcoal additives, the T_b increased by more than 100 K signalizing the difficulty encountered in their burning and the subsequent requirement for longer residence times and higher temperatures to complete the oxidation process [39]. This is consistent with the calculated combustibility indices.

- ignition index:

$$D_i = \frac{DTG_1}{t_1 \bullet t_i} \quad (1)$$

where t_1 – is a corresponding time for DTG_1 (maximum combustion rate)

Table 4
The TGA characteristics for hydrochars.

	T_i°C	DTG_1%/min	T_1°C	DTG_2%/min	T_2°C	T_b°C	R%	D_i%/min^3	D_b%/min^4	S%^{2}/min^2.°C^3	H_f°C
HSS	247	3.943	295	2.776	393	455	43.6	0.0048	$10{\cdot}10^{-5}$	$12{\cdot}10^{-8}$	1048
H1C	239	3.004	301	2.590	400	547	39.4	0.0037	$6{\cdot}10^{-5}$	$8{\cdot}10^{-8}$	1074
H2C	239	2.702	302	2.445	402	566	36.5	0.0033	$5{\cdot}10^{-5}$	$6{\cdot}10^{-8}$	1080
H1F	258	4.897	302	2.729	400	470	41.7	0.0057	$11{\cdot}10^{-5}$	$13{\cdot}10^{-8}$	1075
H2F	257	5.149	303	2.935	400	473	37.3	0.0060	$12{\cdot}10^{-5}$	$13{\cdot}10^{-8}$	1100
H1G	244	4.811	298	2.873	395	453	42.9	0.0059	$12{\cdot}10^{-5}$	$14{\cdot}10^{-8}$	1072
H2G	238	4.811	302	2.443	400	566	43.1	0.0059	$10{\cdot}10^{-5}$	$12{\cdot}10^{-8}$	1080
H1U	239	4.299	302	2.620	393	455	45.1	0.0053	$9{\cdot}10^{-5}$	$13{\cdot}10^{-8}$	1060
H2U	252	5.990	302	3.108	393	456	41.7	0.0072	$14{\cdot}10^{-5}$	$17{\cdot}10^{-8}$	1092

Table 5
Selected oxides identified in hydrochar ash by XRF analysis.

	Na_2O	MgO	Al_2O_3	SiO_2	P_2O_5	K_2O	CaO	TiO_2
SS	0.4648	1.3071	3.9275	7.701	11.3543	1.0587	6.6971	7.248
HSS	0.2455	1.9543	6.2096	11.4197	15.2435	0.6481	8.9942	9.1597
H1C	0.2525	1.8284	5.4377	9.831	13.7452	0.6583	8.5386	8.3348
H2C	0.2035	1.6404	4.9426	8.8541	12.4981	0.6295	8.1213	7.6839
H1F	0.2338	1.9161	5.8212	10.3732	14.6638	0.6577	8.7301	8.9875
H2F	0.2463	1.7219	5.4939	9.6843	13.9729	0.6891	8.3823	8.7811
H1G	0.2616	1.8901	5.9409	11.2864	14.7153	0.7933	8.9002	8.7973
H2G	0.2333	1.8092	5.8511	11.7252	14.0822	0.8667	8.7084	8.5658
H1U	0.3125	1.8906	6.1142	11.223	14.7374	0.6955	9.1626	8.5644
H2U	0.3312	1.8332	6.0785	11.357	14.0109	0.6862	9.3656	8.4688

It measures the ease of the release of volatile matter: the lowest values after the HTC process (0.0033 %·min^{-3}) were determined for samples which combusted the longest e.g. H1C and H2C.

- burnout index

$$D_b = \frac{DTG_1}{\Delta t_{0.5} \bullet t_1 \bullet t_b} \tag{2}$$

where t_b – burnout time, $\Delta t_{0.5}$ - time range of DTG/DTG_1 = 0.5.

The lower values of D_b were found for H1C and H2C suggesting that these samples required less time to complete the combustion process than the others. A larger ignition index was found for H1U suggesting the best performance for ignition.

- combustion index:

$$S = \frac{DTG_1 \bullet DTG_{mean}}{T_i^2 \bullet T_b} \tag{3}$$

S indicated that the highest combustion activity for H1G and H2U which reflects ignition, combustion and burnout properties. The higher value of S shows the superior combustion characteristics of hydrothermally co-carbonized samples. The S values for blends with charcoal are similar to data presented by Song et al. [39,40].

- combustion stability index:

$$H_f = T_1 \bullet \ln\left(\frac{\Delta t_{0.5}}{DTG_{mean}}\right) \tag{4}$$

The H_f index corresponds to the rate and intensity of the combustion processes. Lower values of H_f indicate a more stable combustion process [30,41].

The solid residue (R) found after the combustion process, summarized in Tables 3 and is in line with ash contents performed by proximate analysis.

Hydrothermal carbonization and co-carbonization enhance the combustion characteristics of hydrochar proving that hydrochar combustion performance might be slightly less spontaneous than in the case of sewage sludge. Unfortunately, due to the HTC process, the ash content is accumulates in a much higher quantity in hydrochar than in sewage sludge. For that reason managing the combustion process of fuel with a high ash content can be disrupted by slagging and fouling processes depositing ash on the heating surfaces of the boiler. This can lead to a reduction in of heat transfer and the efficiency of the heating equipment. The resulting problems might be even more severe, including degradation of metallic surfaces by corrosion causing an unexpected blackout [42]. Therefore, the prediction of ash behaviour, in particular prediction of the tendency for slagging and fouling of ash, which results from the chemical composition of the ash, is indeed a very important issue. It might be assessed by the slagging and fouling indices determined and based on oxide contents in the ash. For this purpose, XRF analyses were employed to detect the following oxides in ash: SiO_2, TiO_2, Al_2O_3, P_2O_5 (acids oxide) and Fe_2O_3, Na_2O, K_2O, CaO, MgO (bases oxides) (Table 5).

Table 6
Exploitation risks expressed as slagging and fouling indices.

	R_B	$R_{B/A}$	BAI	S_R	R_S	F_U
SS	16.78	1.39	4.76	33.55	3.65	3.54
HSS	21.00	1.15	10.25	36.22	2.44	1.77
H1C	19.61	1.24	9.15	34.46	2.40	1.91
H2C	18.28	1.28	9.22	33.67	2.34	1.79
H1F	20.53	1.22	10.08	34.57	2.40	1.86
H2F	19.82	1.26	9.39	33.90	2.38	2.01
H1G	20.64	1.16	8.34	36.56	2.36	2.09
H2G	20.18	1.11	7.79	38.06	2.19	2.07
H1U	20.63	1.15	8.50	36.39	2.26	1.98
H2U	20.69	1.14	8.32	36.61	2.05	1.95

The oxides in ash are used to calculate the following indices [43].

- base constituents:

$$R_B = Fe_2O_3 + CaO + MgO + Na_2O + K_2O \tag{5}$$

- base-to-acid ratio:

$$R_{B/A} = \frac{Fe_2O_3 + CaO + MgO + Na_2O + K_2O}{SiO_2 + Al_2O_3 + TiO_2} \tag{6}$$

- bed agglomeration index:

$$BAI = \frac{Fe_2O_3}{Na_2O + K_2O} \tag{7}$$

- slag viscosity index:

$$S_R = \frac{Fe_2O_3 + CaO + MgO + Na_2O + K_2O}{SiO_2 + Al_2O_3 + TiO_2} \tag{8}$$

- slagging index:

$$R_S = R_{B/A} S \tag{9}$$

where S is dry sulphur content (Table 2)

- fouling index:

$$F_U = R_{B/A} \cdot (Na_2O + K_2O) \tag{10}$$

According to Umar et al. [42], slagging tendency occurs with an increasing index ($R_{B/A} < 0.5$ low, $0.5 < R_{B/A} < 0.99$ medium, $1 < R_{B/A} <$

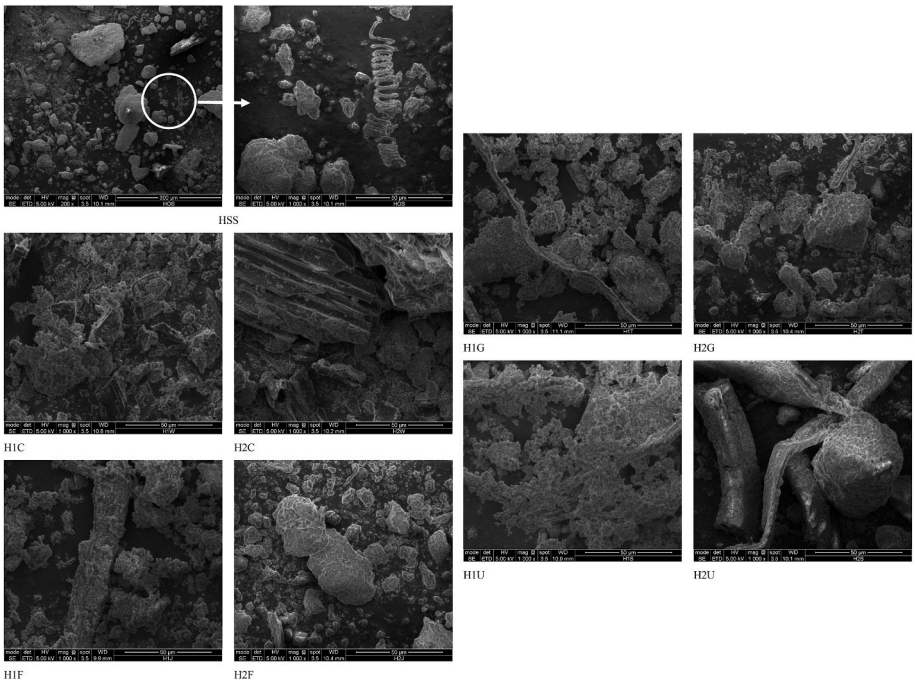

Fig. 7. SEM images of hydrochar without and with organic waste additives.

1.74 high, $R_{B/A} > 1.75$ extremely high tendency). $R_{B/A}$ for the samples, summarized in Table 6, indicate a high tendency for slagging. The BAI index represents a tendency to bed agglomeration during fluidized bed combustion and the risk is high when BAI is below 10. Almost every hydrochars can cause this phenomena. A fouling tendency, based on the F_u index, is expected to be medium ($F_u < 0.6$ low, $0.6 < F_u < 40$ medium, $F_u > 40$ high fouling tendency). Whereas, slag viscosity is significantly high ($S_R > 72$ low, $65 < S_R < 72$ medium, $S_R > 65$ high tendency to form slag). The R_S index indicates propensity for slagging ($R_S < 0.3$ low, slagging tendency occurs for, $0.6 < R_S < 2.0$ medium, $2.0 < R_S < 2.6$ medium, $R_S > 2.6$ extremely high slagging tendency). Hydrochar derived from sewage sludge has an extremely high slagging tendency, whereas co-hydrochars have a slightly better performance suggesting a medium propensity for slagging [44,45].

The reactions occurring during hydrothermal carbonization and co-carbonization caused by temperature, pressure, water agent, and residence time resulted in a degradation of the material. In Fig. 7 SEM images of hydrochar are presented. HSS is shown in 2 magnitudes: 300 and 50 μm depicting the particle of hydrochar without the additive for better comparison with the co-hydrochars. There are many substances incoming to wastewater treatment plants. These are mainly of an organic matter, e.g. human excreta (faeces and urine), human hair, other waste products such as sanitary, food, agriculture, and lignocellulosic, trace chemicals and inorganic solids from medicine and cosmetic products. Although sewage sludge is a pretreated, dewatered material there are always some particles of different origin most likely inorganic or heavy plastics, which do not easily degrade. In Fig. 7, a spirally shaped particle is marked. This is probably made from heavy plastic that is more likely to decompose at 400–800 °C. However, hydrothermal carbonization was performed at 200 °C for 2h, which did not provide severe enough conditions to degrade it. The remaining samples have a much more complex structure due to the use of different additives. Depicted below are co-hydrochars with 10 and 20 % of each additive, including: charcoal, fir, gras, and undersieved fraction of municipal solid mixed waste, respectively. In every case regarding a higher quantity of additives, more particles adhered to the skeleton formed by additives which resulted in accumulation of particles providing higher density of hydrochars inducing improvement in the filtration process as well as in dewaterability.

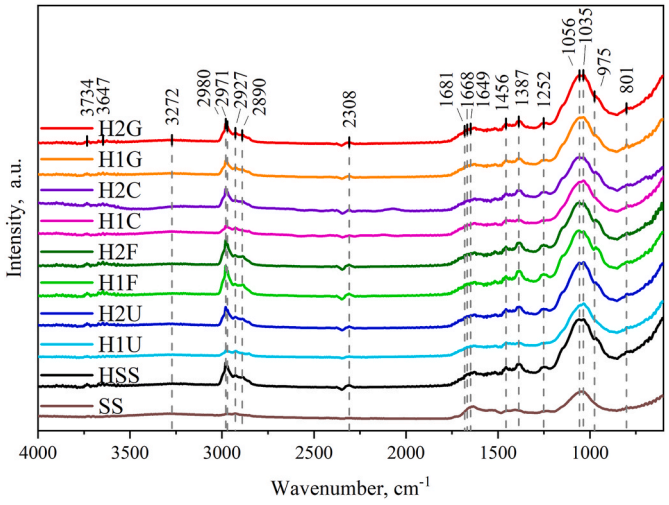

Fig. 8. FTIR spectra of hydrochar without and with organic waste additives.

FTIR spectra of hydrochars and sewage sludge are depicted in Fig. 8. There were no significant changes found in the hydrochars when compared with sewage sludge indicating that the chemical bonds of sewage sludge were not significantly dominated by hydrothermal treatment. Additionally, the shape and character of the spectra of hydrochar with and without additives are very similar. The following chemical bonds were identifie: the wavelength range of 3600 and 3200 cm^{-1} is assigned to the –OH vibration of alcohols, phenols, organic acids and amine hydrogen vibration, most likely in hydroxyl and carboxyl groups. Whereas, 3000–2800 cm^{-1} is allocated to aliphatic hydrocarbons: 2927 and 2890 cm^{-1} represent, most likely, aliphatic carbon C–H and the symmetrical stretching of methylene groups, where higher and broader peaks were found in hydrochars than in sewage sludge [46]. Peaks found in the region of 1800–1350 cm^{-1} are probably attributed to the stretching vibration of C═N amides and the presence of olefins components [47]. It is possible that the peaks of 1681 and 1649 cm^{-1}

Table 7
Specific surface area of hydrochars.

	HSS	H1C	H2C	H1F	H2F	H1G	H2G	H1U	H2U
SSA, m^2/g	15.25	13.22	13.66	15.02	14.72	13.22	13.80	12.46	12.16

Table 8
Characteristics of process water derived from hydrothermal co-carbonization process.

Liquid sample	pH	Conductivity mS/cm	COD mg/L	Phenol mg/L	PO_4–P mg/L	PO_4−3 mg/L	P_2O_5 mg/L	NH_4+ mg/L	Mg mg/L	Ca mg/L	TOC mg/L	Cl free mg/L	Cl total mg/L
HSSL	7.90	12.28	40 690	288	710	2160	1620	2150	250.00	45.00	14 700	38.25	43.00
H1CL	7.46	10.58	41 270	292	690	2120	1580	1750	485.00	40.00	16 200	42.50	45.25
H2CL	8.01	12.21	36 330	317	670	2060	1540	2100	327.50	132.50	15 200	34.50	36.25
H1FL	7.70	10.69	38 120	373	760	2320	1730	1800	265.00	15.00	1 5800	29.75	32.75
H2FL	7.60	9.61	44 470	396	670	2050	1530	1750	330.00	12.00	15 500	34.00	36.75
H1GL	7.51	10.35	45 920	359	730	2240	1670	1800	320.00	16.00	17 200	44.75	50.75
H2GL	7.55	10.49	47 330	421	830	2530	1890	2250	435.00	19.00	17 500	41.00	43.00
H1UL	7.72	12.07	41 650	292	730	2230	1670	1650	477.50	12.00	14 100	36.75	38.00
H2UL	8.57	13.70	35 710	307	740	2270	1690	2350	425.00	15.00	15 100	39.25	45.00

corresponds to the stretching vibrations of C═O and C═C groups in ketones and amide groups [19,48]. The wavelength of 1456 cm^{-1} corresponded to aromatic C═C stretching and to the existence of a carboxylic group in the hydrochar. Whereas, peaks in the range of 1400 and 1200 cm^{-1}, in particular 1387, were a result of the degradation of lignocellulosic biomass [19]. At 1252 cm^{-1} is a peak representing C–O–C stretching [49]. The polysaccharides can be found in the region of 1100–1000 cm^{-1} after decomposition of sewage sludge caused by the hydrothermal carbonization process. The stronger and broader peaks at 1056 or 1035 cm^{-1} are probably connected to carboxylic acids or alcohols (–C–OH) and C–O bond of primary hydroxyl or Si–O stretching and Si–O–Si bonds. Between 1200 and 800 cm^{-1} the mineral components can be assigned [50].

Accordingly, the specific surface area for all hydrochars are summarized in Table 7. The SSA values for co-hydrochars are slightly lower or at the same level as hydrochar derived from sewage sludge, indicating that additives did not enhanced this parameter. Therefore, other more advanced processes should be employed for creating a more porous and sorptive structure of co-hydrochar.

Besides hydrochar, there is also a large volume of process water (HTCL) derived from hydrothermal treatment, in which the characteristics strongly depends on the process conditions and feedstock composition. For instance, the hydrothermal co-carbonization process, in particular, of both feedstock and organic waste additives. The main process water characteristics are summarized in Table 8.

The pH of the HSSL is slightly alkaline at 7.9, which is similar to other studies [9]. The lignocellulosic additives reduce this slightly, but only the 20 % undersieved fraction of municipal solid waste sample raised the pH to 8.57.

Conductivity, for HSSL is 12.28 mS/cm and this decreases with the addition of lignocellulosic and charcoal, by about 28 % with 20 % of fir addition. With 20 % undersieved fraction of municipal solid waste, there was a slight increase of this parameter indicating that process water consists of some polar compounds.

The COD level for HSSL is significantly high (40 690 mg/L) confirming significant pollution of process water from sewage sludge. The additives change this slightly, but not for any specific trend: COD values are still high, within the range of 35 710 (H2UL) to 47 330 mg/L (H2GL), depending on the quantity and kind of additives used.

Phenol rose for every additives, but the highest values were reached for H2G and H2F, mainly caused by increased lignin dissolution in the process water. For phosphorous compounds, the same trend was observed: the highest values were measured for H2G and the lowest for H2F and H2C. Ammonia content decreased by 15–25 % with 10 % of every additives: for instance, 20 % undersieved fraction of municipal solid waste effected a slight increase when compared to hydrochar without additives.

TOC levels were slightly raised with the addition of additives, e.g. it increased by about 20 % with the addition of straw. The same trend was observed for chlorine content, where also 10 % of charcoal resulted in an increase.

The detailed and profound analyses on the post-processing liquid derived from the hydrothermally treatment of this particular sewage sludge was published by Czerwińska et al. [51], where membrane filtration processes (ultrafiltration, nanofiltration and double nanofiltration) and other selected advanced processes (coagulation, ultrasonication and chlorination) were implemented in order to effectively purify this liquid. Moreover, the results of distillation as an effective purification method of the post-processing water was also published in Ref. [52].

Concluding, the highly organic loads in the process waters derived from hydrothermal co-carbonization are promising for energy recovery through anaerobic digestion or methanogenesis. Moreover, the presence of essential plant nutrients suggest it might also be used as a liquid fertilizer. Nevertheless, the process water requires an effective treatment, before implementing this method on an industrial scale.

4. Conclusions

Hydrothermal co-carbonization of sewage sludge and organic waste led to improvement of the dewaterability and fuel properties of hydrochars. The organic additives caused the decrease of moisture content in pressure filtration cakes, lower the pressure filtration time and capillary suction time, in particular 20 % of addition. An increase in the higher heating value, carbon and fixed carbon contents was found giving the optimal fuel properties when compared to hydrochars of sewage sludge. The combustibility indexes confirmed slightly easier and more stable combustion compared to hydrothermally treated sludge without an additive. The addition of charcoal increased the higher heating value and prolonged the time of combustion. The most optimal results of combustion performance regarding S and H_f and D_i indices were achieved for the 20 % undersieved fraction of municipal solid waste. Moreover, the modified morphological structure was observed, but the specific surface area indicates the necessity for some further enhancement before being used as a potential adsorbent. The process water characteristics indicate the potential for nutrients and energy recovery after economic and environmental assessment.

Data availability

Data are available in https://doi.org/10.58032/AGH/C79CH7.

CRediT authorship contribution statement

Małgorzata Wilk: Writing – review & editing, Writing – original draft, Visualization, Validation, Supervision, Resources, Project administration, Methodology, Investigation, Funding acquisition, Formal analysis, Data curation, Conceptualization. **Maciej Śliz:** Writing – original draft, Visualization, Validation, Resources, Methodology, Investigation, Formal analysis, Data curation. **Klaudia Czerwińska:** Validation, Methodology, Investigation, Formal analysis, Data curation. **Marcin Gajek:** Validation, Resources, Methodology, Investigation. **Izabela Kalemba-Rec:** Visualization, Validation, Methodology, Investigation, Conceptualization.

Declaration of competing interest

The authors declare that they have no known competing financial interests or personal relationships that could have appeared to influence the work reported in this paper.

Acknowledgements

The research was founded by the National Science Centre Poland under the project no. 2021/41/B/ST8/01815. The authors would like to express their thanks to the proprietor of the experimental apparatus EKOPROD Ltd. in Bytom. This work was presented during the 18th Conference on the Sustainable Development of Energy, Water and Environment Systems – SDEWES, held in hybrid mode from September 24–29, 2023 in Dubrovnik, Croatia. The authors also wish to thank Prof. Lidia Lombardi (Niccolo Cusano University, Rome, Italy) for her help with supplying the research material.

References

[1] H.B. Sharma, S. Venna, B.K. Dubey, Resource recovery and circular economy approach in organic waste management using hydrothermal carbonization, in: Clean Energy Resour. Recover., Elsevier, 2021, pp. 313–326, https://doi.org/10.1016/B978-0-323-85223-4.00003-8.

[2] L.P. Padhye, E.R. Bandala, B. Wijesiri, A. Goonetilleke, N. Bolan, Hydrochar: a promising step towards achieving a circular economy and sustainable development goals, Front. Chem. Eng. 4 (2022), https://doi.org/10.3389/fceng.2022.867228.

[3] P.A. Østergaard, N. Duic, Y. Noorollahi, H. Mikulcic, S. Kalogirou, Sustainable development using renewable energy technology, Renew. Energy 146 (2020) 2430–2437, https://doi.org/10.1016/j.renene.2019.08.094.

[4] P.A. Østergaard, N. Duic, Y. Noorollahi, S.A. Kalogirou, Recent advances in renewable energy technology for the energy transition, Renew. Energy 179 (2021) 877–884, https://doi.org/10.1016/j.renene.2021.07.111.

[5] M. Cavali, N. Libardi Junior, J.D. de Sena, A.L. Woiciechowski, C.R. Soccol, P. Belli Filho, R. Bayard, H. Benbelkacem, A.B. de Castilhos Junior, A review on hydrothermal carbonization of potential biomass wastes, characterization and environmental applications of hydrochar, and biorefinery perspectives of the process, Sci. Total Environ. 857 (2023) 159627, https://doi.org/10.1016/j.scitotenv.2022.159627.

[6] M. Bagheri, E. Wetterlund, Introducing hydrothermal carbonization to sewage sludge treatment systems—a way of improving energy recovery and economic performance? Waste Manag. 170 (2023) 131–143, https://doi.org/10.1016/j.wasman.2023.08.006.

[7] G. Przydatek, A.K. Wota, Analysis of the comprehensive management of sewage sludge in Poland, J. Mater. Cycles Waste Manag. 22 (2020) 80–88, https://doi.org/10.1007/s10163-019-00937-y.

[8] M. Sharma, A. Yadav, M.K. Mandal, S. Pandey, S. Pal, H. Chaudhuri, S. Chakrabarti, K.K. Dubey, Wastewater treatment and sludge management strategies for environmental sustainability, in: Circ. Econ. Sustain., Elsevier, 2022, pp. 97–112, https://doi.org/10.1016/B978-0-12-821664-4.00027-3.

[9] M. Wilk, A novel method of sewage sludge pre-Treatment-HTC, E3S Web Conf. 10 (2016) 1–6, https://doi.org/10.1051/e3sconf/20161000103.

[10] M. Malhotra, A. Garg, Hydrothermal carbonization of sewage sludge: optimization of operating conditions using design of experiment approach and evaluation of resource recovery potential, J. Environ. Chem. Eng. 11 (2023) 109507, https://doi.org/10.1016/j.jece.2023.109507.

[11] S.Z. Roslan, S.F. Zainudin, A. Mohd Aris, K.B. Chin, M. Musa, A.R. Mohamad Daud, S.S.A. Syed Hassan, Hydrothermal carbonization of sewage sludge into solid biofuel: influences of process conditions on the energetic properties of hydrochar, Energies 16 (2023) 2483, https://doi.org/10.3390/en16052483.

[12] K. Czerwińska, M. Śliz, M. Wilk, Hydrothermal carbonization process: fundamentals, main parameter characteristics and possible applications including an effective method of SARS-CoV-2 mitigation in sewage sludge, A review, Renew. Sustain. Energy Rev. 154 (2022) 111873, https://doi.org/10.1016/j.rser.2021.111873.

[13] T. Wang, Y. Zhai, Y. Zhu, C. Li, G. Zeng, A review of the hydrothermal carbonization of biomass waste for hydrochar formation: process conditions, fundamentals, and physicochemical properties, Renew. Sustain. Energy Rev. 90 (2018) 223–247, https://doi.org/10.1016/j.rser.2018.03.071.

[14] M. Wilk, M. Gajek, M. Śliz, K. Czerwińska, L. Lombardi, Hydrothermal carbonization process of digestate from sewage sludge: chemical and physical properties of hydrochar in terms of energy application, Energies 15 (2022) 6499, https://doi.org/10.3390/en15186499.

[15] M. Wilk, M. Śliz, B. Lubieniecki, Hydrothermal co-carbonization of sewage sludge and fuel additives: combustion performance of hydrochar, Renew. Energy 178 (2021) 1046–1056, https://doi.org/10.1016/j.renene.2021.06.101.

[16] X. Lu, X. Ma, X. Chen, Co-hydrothermal carbonization of sewage sludge and lignocellulosic biomass: fuel properties and heavy metal transformation behaviour of hydrochars, Energy 221 (2021) 119896, https://doi.org/10.1016/j.energy.2021.119896.

[17] X. Lu, X. Ma, Z. Qin, C. Ke, L. Chen, X. Chen, Co-hydrothermal carbonization of sewage sludge with wood chip: fuel properties and heavy metal transformation behavior of hydrochars, Energy Fuels 35 (2021) 15790–15801, https://doi.org/10.1021/acs.energyfuels.1c02145.

[18] C. Zhang, C. Zheng, X. Ma, Y. Zhou, J. Wu, Co-hydrothermal carbonization of sewage sludge and banana stalk: fuel properties of hydrochar and environmental risks of heavy metals, J. Environ. Chem. Eng. 9 (2021) 106051, https://doi.org/10.1016/J.JECE.2021.106051.

[19] X. Zhang, L. Zhang, A. Li, Hydrothermal co-carbonization of sewage sludge and pinewood sawdust for nutrient-rich hydrochar production: synergistic effects and products characterization, J. Environ. Manag. 201 (2017) 52–62, https://doi.org/10.1016/j.jenvman.2017.06.018.

[20] C. He, Z. Zhang, C. Ge, W. Liu, Y. Tang, X. Zhuang, R. Qiu, Synergistic effect of hydrothermal co-carbonization of sewage sludge with fruit and agricultural wastes on hydrochar fuel quality and combustion behavior, Waste Manag. 100 (2019) 171–181, https://doi.org/10.1016/j.wasman.2019.09.018.

[21] C. Peng, Y. Zhai, Y. Zhu, T. Wang, B. Xu, T. Wang, C. Li, G. Zeng, Investigation of the structure and reaction pathway of char obtained from sewage sludge with biomass wastes, using hydrothermal treatment, J. Clean. Prod. 166 (2017) 114–123, https://doi.org/10.1016/j.jclepro.2017.07.108.

[22] Q. Wang, S. Wu, D. Cui, H. Zhou, D. Wu, S. Pan, F. Xu, Z. Wang, Co-hydrothermal carbonization of organic solid wastes to hydrochar as potential fuel: a review, Sci. Total Environ. 850 (2022) 158034, https://doi.org/10.1016/j.scitotenv.2022.158034.

[23] R. Wang, K. Lin, P. Peng, Z. Lin, Z. Zhao, Q. Yin, L. Ge, Energy yield optimization of co-hydrothermal carbonization of sewage sludge and pinewood sawdust coupled with anaerobic digestion of the wastewater byproduct, Fuel 326 (2022) 125025, https://doi.org/10.1016/j.fuel.2022.125025.

[24] K.R. Parmar, A.E. Brown, J.M. Hammerton, M.A. Camargo-Valero, L.A. Fletcher, A. B. Ross, Co-processing lignocellulosic biomass and sewage digestate by hydrothermal carbonisation: influence of blending on product quality, Energies 15 (2022) 1418, https://doi.org/10.3390/en15041418.

[25] O.S. Djandja, S. Kang, Z. Huang, J. Li, J. Feng, Z. Tan, A.A. Salami, B.G. Lougou, Machine learning prediction of fuel properties of hydrochar from co-hydrothermal carbonization of sewage sludge and lignocellulosic biomass, Energy 271 (2023) 126968, https://doi.org/10.1016/j.energy.2023.126968.

[26] M. Bardhan, T.M. Novera, M. Tabassum, M.A. Islam, M.A. Islam, B.H. Hameed, Co-hydrothermal carbonization of different feedstocks to hydrochar as potential energy for the future world: a review, J. Clean. Prod. 298 (2021) 126734, https://doi.org/10.1016/j.jclepro.2021.126734.

[27] S. Fakudze, J. Chen, A critical review on co-hydrothermal carbonization of biomass and fossil-based feedstocks for cleaner solid fuel production: synergistic effects and environmental benefits, Chem. Eng. J. 457 (2023) 141004, https://doi.org/10.1016/j.cej.2022.141004.

[28] C. Zhang, X. Ma, C. Zheng, T. Huang, X. Lu, Y. Tian, Co-Hydrothermal carbonization of water hyacinth and sewage sludge: effects of aqueous phase recirculation on the characteristics of hydrochar, Energy Fuels 34 (2020) 14147–14158, https://doi.org/10.1021/acs.energyfuels.0c01991.

[29] S. Mahata, S.R. Periyavaram, N.K. Akkupalli, S. Srivastava, C. Matli, A review on Co-Hydrothermal carbonization of sludge: effect of process parameters, reaction pathway, and pollutant transport, J. Energy Inst. 110 (2023) 101340, https://doi.org/10.1016/j.joei.2023.101340.

[30] G. Shan, W. Li, S. Bao, Y. Li, W. Tan, Co-hydrothermal carbonization of agricultural waste and sewage sludge for product quality improvement: fuel properties of hydrochar and fertilizer quality of aqueous phase, J. Environ. Manag. 326 (2023) 116781, https://doi.org/10.1016/j.jenvman.2022.116781.

[31] M. Śliz, F. Tuci, K. Czerwińska, S. Fabrizi, L. Lombardi, M. Wilk, Hydrothermal carbonization of the wet fraction from mixed municipal solid waste: hydrochar characteristics and energy balance, Waste Manag. 151 (2022) 39–48, https://doi.org/10.1016/j.wasman.2022.07.029.

[32] D.W. Rutherford, C.T. Chiou, D.E. Kile, Influence of soil organic matter composition on the partition of organic compounds, Environ. Sci. Technol. 26 (1992) 336–340, https://doi.org/10.1021/es00026a014.

[33] B. Wu, C.M. Taylor, D.R.U. Knappe, M.A. Nanny, M.A. Barlaz, Factors controlling alkylbenzene sorption to municipal solid waste, Environ. Sci. Technol. 35 (2001) 4569–4576, https://doi.org/10.1021/es010893a.
[34] L. Li, Y. Wang, J. Xu, J.R.V. Flora, S. Hoque, N.D. Berge, Quantifying the sensitivity of feedstock properties and process conditions on hydrochar yield, carbon content, and energy content, Bioresour. Technol. 262 (2018) 284–293, https://doi.org/10.1016/j.biortech.2018.04.066.
[35] J. Wielinski, C. Müller, A. Voegelin, E. Morgenroth, R. Kaegi, Combustion of sewage sludge: kinetics and speciation of the combustible, Energy Fuels 32 (2018) 10656–10667, https://doi.org/10.1021/acs.energyfuels.8b02106.
[36] C. He, A. Giannis, J.Y. Wang, Conversion of sewage sludge to clean solid fuel using hydrothermal carbonization: hydrochar fuel characteristics and combustion behavior, Appl. Energy 111 (2013) 257–266, https://doi.org/10.1016/j.apenergy.2013.04.084.
[37] OBWIESZCZENIE MINISTRA KLIMATU I Ś RODOWISKA1) z dnia 18 listopada 2022 r, w Sprawie Ogłoszenia Jednolitego Tekstu Rozporządzenia Ministra Środowiska W Sprawie Stosowania Komunalnych Osadów Ściekowych, Journal of Laws of the Republic of Poland, Poland, 2023. https://isap.sejm.gov.pl/isap.nsf/DocDetails.xsp?id=WDU20230000023.
[38] Strategia postępowania z komunalnymi osadami ściekowymi na lata 2019-2022. https://www.gov.pl/attachment/2846e2b3-68c7-46eb-b36e-7643e81efd9a, 2018.
[39] M. Mureddu, F. Dessì, A. Orsini, F. Ferrara, A. Pettinau, Air- and oxygen-blown characterization of coal and biomass by thermogravimetric analysis, Fuel 212 (2018) 626–637, https://doi.org/10.1016/j.fuel.2017.10.005.
[40] C.-Z. Song, J.-H. Wen, Y.-Y. Li, H. Dan, X.-Y. Shi, S. Xin, Thermogravimetric Assessment of Combustion Characteristics of Blends of Lignite Coals with Coal Gangue, 105, 2017, pp. 490–495, https://doi.org/10.2991/mme-16.2017.67.
[41] S. Paiboonudomkarn, K. Wantala, Y. Lubphoo, R. Khunphonoi, Conversion of sewage sludge from industrial wastewater treatment to solid fuel through hydrothermal carbonization process, Mater. Today Proc. 75 (2023) 85–90, https://doi.org/10.1016/j.matpr.2022.11.107.
[42] D.F. Umar, Z. Zulfahmi, T. Suseno, S. Suganal, N. Madiutomo, L. Setiawan, E. A. Daranin, G. Gunawan, Hydrothermal dewatering of low-grade coal: product evaluation and primary component analysis of ash deposition, Heliyon 9 (2023) e22022, https://doi.org/10.1016/j.heliyon.2023.e22022.
[43] C. Zhu, H. Tu, Y. Bai, D. Ma, Y. Zhao, Evaluation of slagging and fouling characteristics during Zhundong coal co-firing with a Si/Al dominated low rank coal, Fuel 254 (2019) 115730, https://doi.org/10.1016/j.fuel.2019.115730.
[44] B. Kamara, D.V. Von Kallon, P.M. Mashinini, Fouling and slagging investigation on ash derived from sasol coal using ICP and XRF analytical techniques, Appl. Sci. 12 (2022) 11560, https://doi.org/10.3390/app122211560.
[45] K.J. Abioye, N.Y. Harun, S. Sufian, M. Yusuf, A.H. Jagaba, B.C. Ekeoma, H. Kamyab, S. Sikiru, S. Waqas, H. Ibrahim, A review of biomass ash related problems: mechanism, solution, and outlook, J. Energy Inst. 112 (2024) 101490, https://doi.org/10.1016/j.joei.2023.101490.
[46] X. Zheng, Z. Jiang, Z. Ying, J. Song, W. Chen, B. Wang, Role of feedstock properties and hydrothermal carbonization conditions on fuel properties of sewage sludge-derived hydrochar using multiple linear regression technique, Fuel 271 (2020) 117609, https://doi.org/10.1016/j.fuel.2020.117609.
[47] X. Zhuang, H. Zhan, Y. Song, C. He, Y. Huang, X. Yin, C. Wu, Insights into the evolution of chemical structures in lignocellulose and non-lignocellulose biowastes during hydrothermal carbonization (HTC), Fuel 236 (2019) 960–974, https://doi.org/10.1016/j.fuel.2018.09.019.
[48] M. Cavali, H. Benbelkacem, B. Kim, R. Bayard, N. Libardi Junior, D. Gonzaga Domingos, A.L. Woiciechowski, A.B. de Castilhos Junior, Co-hydrothermal carbonization of pine residual sawdust and non-dewatered sewage sludge – effect of reaction conditions on hydrochar characteristics, J. Environ. Manag. 340 (2023) 117994, https://doi.org/10.1016/j.jenvman.2023.117994.
[49] S. Piboonudomkarn, P. Khemthong, S. Youngjan, K. Wantala, V. Tanboonchuy, Y. Lubphoo, R. Khunphonoi, Co-hydrothermally carbonized sewage sludge and lignocellulosic biomass: an efficiently renewable solid fuel, Arab. J. Chem. 16 (2023) 105315, https://doi.org/10.1016/j.arabjc.2023.105315.
[50] G.K. Parshetti, Z. Liu, A. Jain, M.P. Srinivasan, R. Balasubramanian, Hydrothermal carbonization of sewage sludge for energy production with coal, Fuel 111 (2013) 201–210, https://doi.org/10.1016/j.fuel.2013.04.052.
[51] K. Czerwińska, A. Marszałek, E. Kudlek, M. Śliz, M. Dudziak, M. Wilk, The treatment of post-processing liquid from the hydrothermal carbonization of sewage sludge, Sci. Total Environ. 885 (2023) 163858, https://doi.org/10.1016/j.scitotenv.2023.163858.
[52] K. Czerwińska, M. Śliz, M. Wilk, Thermal disposal of post-processing water derived from the hydrothermal carbonization process of sewage sludge, Waste and Biomass Valorization 15 (2024) 1671–1680, https://doi.org/10.1007/s12649-023-02162-z.